

HIGH-RESOLUTION THERMAL FACE DATASET FOR FACE AND EXPRESSION RECOGNITION

Marcin Kowalski, Artur Grudziń

Military University of Technology, Institute of Optoelectronics, Gen. W. Urbanowicza 2, 00-908 Warsaw, Poland

(✉ marcin.kowalski@wat.edu.pl, +48 261 83 9353, artur.grudzien@wat.edu.pl)

Abstract

Development of facial recognition or expression recognition algorithms requires input data to thoroughly test the performance of algorithms in various conditions. Researchers are developing various methods to face challenges like illumination, pose and expression changes, as well as facial disguises. In this paper, we propose and establish a dataset of thermal facial images, which contains a set of neutral images in various poses as well as a set of facial images with different posed expressions collected with a thermal infrared camera. Since the properties of face in the thermal domain strongly depend on time, in order to show the impact of aging, collection of the dataset has been repeated and a corresponding set of data is provided. The paper describes the measurement methodology and database structure. We present baseline results of processing using state-of-the-art facial descriptors combined with distance metrics for thermal face re-identification. Three selected local descriptors, a histogram of oriented gradients, local binary patterns and local derivative patterns are used for elementary assessment of the database. The dataset offers a wide range of capabilities – from thermal face recognition to thermal expression recognition.

Keywords: face database, biometrics, thermal face recognition, infrared, face re-identification.

© 2018 Polish Academy of Sciences. All rights reserved

1. Introduction

Face recognition systems operating in the visible domain have reached a significant level of maturity which enables their wide commercial use. Also, due to a low cost of visible-range cameras, investigations on face recognition have been directed towards this spectrum [1, 2]. However, visible spectrum images strongly depend on ambient conditions since they rely on reflectivity of surfaces. The dependence on reflectivity makes them vulnerable to various attacks, like a presentation attack, and it requires additional methods to uniformly distribute illumination on the surface of the face. There are several challenges like illumination [3], pose [4], facial disguises and changes of facial expression, that are still unresolved [5]. The research community has made a great effort to face those challenges by developing more complex solutions. One of the promising directions is exploration of the infrared range of radiation [6].

According to the Planck's law each body being in the thermal equilibrium emits radiation in a broad spectral range [9]. Most of the heat energy is emitted in the LWIR range. The temperature

differences on the face surface correspond to the differences of energy radiated in a broad radiation range. Passive cameras assign the temperature differences to the differences in the radiated energies in their spectral ranges per unit surface [10].

A thermal infrared image of the human face presents its unique heat-signature which can be used as a pattern for recognition [7]. Practical application of thermal face recognition is more complex since the energy received by a thermal camera does not only depend on the properties of measured body (emissivity) but also on the sum of the energies radiated by different elements of the scene captured by the camera, atmosphere characteristics and performance of the imager.

The use of infrared images for automatic face recognition is not free of challenges. Thermal face imaging is sensitive to the emotional, physical and health conditions of the subject [8, 9]. Moreover, the properties of face depend on temperature of body, environment and occlusions present on the face like scarfs, glasses or any disguise accessories that alter the emitted heat pattern.

Face recognition based on infrared thermography remains not fully covered an area, especially in the context of qualitative and quantitative influence of time and environmental impacts. Development and assessment of face recognition algorithms, in particular based on the machine learning paradigm require a large number of samples to train and test models. Most of the existing datasets were collected using imagers offering out-of-date parameters. Moreover, the datasets consist of sample images collected once during a single acquisition. The impact of aging and varying conditions cannot be investigated using available datasets. It is of particular importance to collect and distribute a dataset of facial images acquired repeatedly after a specific period of time using state-of-the-art equipment.

The aim of this paper is to present a high-resolution database of thermal facial images acquired in similar, controlled conditions using a state-of-the-art long-wavelength infrared imager. The dataset contains images presenting faces in a neutral frontal position, in various head positions as well as frontal face images expressing various emotions. The measurement process, database structure and experiment scenarios are described. The dataset has been evaluated in three re-identification scenarios. Three descriptors have been selected to provide baseline recognition results and have been studied in conjunction with seven distance metrics. The paper presents a review of existing thermal face datasets, an overall description of the recognition process and feature extraction methods.

2. Public datasets

Development of processing methods and algorithms requires input data to test and validate their performance in various conditions. Datasets are required to evaluate algorithms as well as to train machine learning or deep learning models. Images may be acquired in various conditions as well as in different states of the subject – moving or in a standoff position. It is highly desirable to collect many datasets covering various scenarios and to compare results of the experiments using repeatable conditions.

One of the methods to compare results is to use public and freely available sets of data. Researchers may use infrared face datasets which offer substantial sets of images. The main and most known databases which contain face images in the infrared spectrum are following:

- a) Equinox [12] – 320×240 -pixel images of 90 subjects;
- b) SCFace [13] – 130 subjects and the total of 4160 images;
- c) Carl Database [13, 14] – 160×120 -pixel images of 41 persons;
- d) Iris thermal/visible face database [16] – 4228 pairs of 320×240 -pixel images;

- e) University of Notre Dame (UND) [17] – 320×240 -pixel images of 241 subjects;
- f) The Laval University thermal IR face motion database [18] – 640×512 -pixel images of 200 subjects.
- g) Natural Visible and Infrared Facial Expression database (USTC-NVIE) [19] – around 100 subjects with images of 320×240 -pixel resolution.

It should be stressed that the authors of the databases focused their attention on different aspects. As an effect, the datasets differ in content and methodology. It is worth mentioning that most of the currently available datasets contain images of relatively low resolution and were captured using imagers with a low value of *minimum resolvable temperature difference* (MRTD), which is the critical parameter describing a sensor's ability to distinguish temperatures. The current state-of-the-art equipment offers resolution of at least 640×480 -pixels and MRTD below 50 mK. What is equally important, collection of a dataset should be repeated after some period of time since aging and different ambient conditions may significantly influence the performance. Therefore, it is justified to collect datasets using current equipment and updated methodologies.

3. Database acquisition

The presented dataset consists of 2 sets of images, collected initially and after 12 months. Each set consists of 30 subsets of images collected from 30 persons, including 10 sets of images of subjects wearing glasses. Each of the 30 datasets contains 24 or 12 images of a subject's face depending on whether the subject is wearing glasses or not, respectively. These images present the subject with various head poses and showing various expressions. The dataset offers a wide range of capabilities – from thermal face recognition to thermal expression recognition. The expression recognition in the thermal domain has received relatively little attention compared with the visible-light expression recognition, thus this topic remains attractive for researchers.

Images from each set present a subject's face in frontal as well as various head positions and showing various expressions. Every set consists of three frontal images presenting the face in the upright position, four images presenting the face in various head positions (looking down, looking left (30 degrees), looking right (30 degrees), looking up) and five frontal-face images presenting various expressions of a subject. The set of expressions includes a subject smiling, sad, surprised, angry and with eyes closed.

This set of images should provide a sufficient number of images and test cases. A sample set of 10 IR images is presented in Fig. 1.

All the measurements were taken indoors. A subject was sitting on a chair in front of the camera at a distance of 1.5 m. The camera was placed at a height of 1.2 m above the floor. Ambient temperature during each of the measurement sessions was controlled using a thermometer and stabilized using an air conditioning system. In order to ensure a uniform background of images, the camera was directed towards the wall covered with cotton fabric. The fabric was aimed to reduce the non-uniformity of wall as well as to eliminate reflections.

During the experiment a subject sitting in front of the camera was performing specific actions guided by a person supervising the measurement process. In order to assure that the angle of head rotation is always the same, numbered markers were installed on the walls and on the floor of the room. A subject was asked to move or rotate the head towards and look at a marker. All the expressions were elicited by asking subjects to perform a series of emotional expressions in front of a camera. Subjects wearing glasses were asked to perform in two measurement sessions where

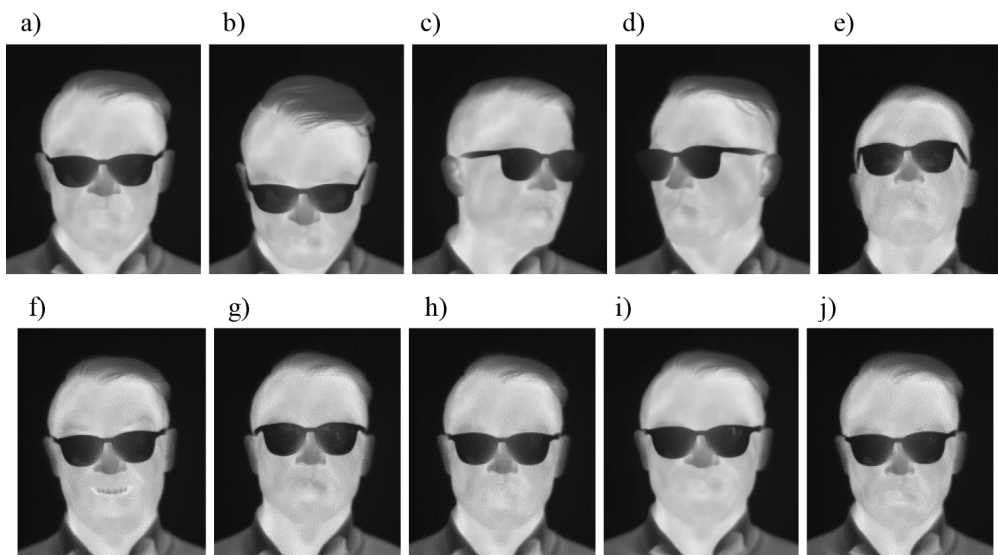


Fig. 1. A dataset of thermal images presenting a face with various positions and expressions: a) upright; b) looking down; c) looking left (30 degrees); d) looking right (30 degrees); e) looking up; f) smiling; g) sad; h) surprised; i) angry; j) eyes closed.

the first one was without and the second with glasses. In order not to exhaust the participant, each measurement session took no longer than 3 minutes.

Face recognition with the thermal infrared camera might be achieved by analysing the relative temperature distribution on the surface of a face. The fundamental parameter of infrared cameras that describes their ability to differentiate temperatures is the *noise equivalent temperature difference* (NETD). The parameter directly defines the ability of a camera to detect shapes of an object. Infrared cameras equipped with uncooled micro-bolometer focal plane arrays offer NETD values between 40 and 130 mK, whereas imagers with cooled detection units have an NETD value below 20 mK. During the acquisition process of thermal infrared images, a camera equipped with 640×480 -pixel micro-bolometer array of NETD < 50 mK was used. The technical specification of the sensor is provided in Table 1.

Table 1. Parameters of the FLIR P640 camera.

Parameters	Values
Detection unit	FPA (focal plane array), MCT (mercury cadmium telluride)
Resolution	640×480 pixels
Field of View (FOV)	$11^\circ \times 8^\circ$
spectral range	$7.7 \mu\text{m} \div 11.5 \mu\text{m}$
NETD	< 50 mK

During all the measurement sessions, the thermal camera has operated in the auto-calibration mode.

4. Evaluation methodology

The presented dataset has been evaluated in terms of its usability for face recognition and expression recognition. In order to quantitatively and qualitatively validate the dataset, a set of state-of-the-art algorithms have been selected.

4.1. Data processing

The mathematical description of face relies on the values derived from a facial image. The derived values, often referred to as features, should provide non-redundant information, facilitating the learning process. Since a variety of face descriptors is known, selection of the most suitable type of features for a chosen task remains a challenge.

There are several various descriptors which differ in performance depending on the spectral domain. The visible-domain face recognition is very often based on appearance-based methods, such as PCA (*Principal Component Analysis*) [12], LDA (*Linear Discriminant Analysis*) [21], and ICA (*Independent Component Analysis*) [22], which project face images into a subspace. Other frameworks use a local-matching approach such as *Local Binary Pattern* (LBP) [23, 24], Gabor Jet Descriptors [25], histograms of Weber Linear Descriptor features [26] and *histograms of oriented gradients* (HOGs) [27]. In these approaches, a facial image is divided into blocks to extract descriptors. Finally, global matching approaches such as *Scale Invariant Feature Transform* (SIFT) and *Speeded-Up Robust Features* (SURF) [28, 29] are used.

Our evaluation methodology is based on using state-of-the-art methods and algorithms to assess the usability of a dataset for thermal face verification (re-identification). We selected and examined three state-of-the-art local feature extraction methods – a histogram of oriented gradients, local binary patterns and local derivative patterns, together with a set of metrics to compare and assess effectiveness of the presented dataset.

The first descriptor considered in this paper was introduced by McConnell in 1986 [30], but its wide usage started after the presentation by Dalal and Triggs at the CVPR conference in 2005 [1]. Dalal and Triggs were the first that successfully applied HOG to human detection. This was an insight for researchers to use HOG for the face representation and the face recognition [32–34]. The HOG feature is a local descriptor of the orientations of the image gradients around the central point of an image. Each descriptor is a package of histograms of pixel orientations extracted by calculation of their gradients.

Local binary pattern (LBP) is another local operator often used for description of facial features. LBP was originally introduced by Ojala *et al.* in [23, 24] as a method to describe textures. Several researchers proposed extensions to the traditional version of LBP. Tan and Triggs [37] extended LBPs to *Local Ternary Patterns* (LTPs), Ahonen *et al.* [36] introduced *Soft Histogram for Local Binary Patterns* (SLBPs), Heikkilä *et al.* [37] proposed *Center-Symmetric Local Binary Patterns* (CSLBPs). Other approaches combining LBP with other methods were further introduced, like *Histograms of Local Variation Patterns* (MHLVPs) or *Local Gabor Binary Pattern Histogram Sequence* (LGBPHS) proposed by Zhang *et al.* [38] and [39].

Zhang *et al.* proposed a new local feature descriptor called *Local Derivative Patterns* (LDP) in 2010 [40]. This new descriptor is able to capture a change of derivative directions among local neighbours and encode the turning point in a given direction. The LDP is based on using high-order local patterns for the face representation [42, 43]. This is the third descriptor compared in the scope of this study.

Detailed mathematical descriptions of HOG, LBP and LDP are provided in [1, 23] and [40], respectively. It should be noticed that HOG, as well as LBP and LDP is calculated around a

selected specific central point of the cell or block of an image. Shape information of tightly cropped images may be lost, thus to avoid losing this information the face detection and cropping should include an extra margin of pixels around the patch that contains background pixels. The images used in the experiment are loosely cropped in order to include relevant information as well as additional background pixels.

The processing scheme of face re-identification is presented in Fig. 2. Two sample images are pre-processed before face detection and segmentation using several various techniques, including normalization techniques, bad-pixel filtering [44] and adaptive filtering [45] in order to remove speckles and other undesirable elements of image. The next stage, face detection is performed using the Viola-Jones algorithm. It is the most common face detection algorithm, based on Haar features and the AdaBoost machine learning algorithm [46]. The feature extraction is the last step before comparison of samples.



Fig. 2. A processing scheme of face re-identification.

Since the re-identification process involves two samples to assess the similarity or validate the identity of a person, comparison of samples (matching) is made based on distance metrics. The matching is a process of comparing the query features against the features of stored samples to generate a score. We compare feature vectors computed from both sample images using distance metrics against a threshold calculated on the entire dataset. A set of metrics including Chebyshev distance, city block (L1), correlation distance, cosine distance, Euclidean distance, Spearman distance, and Mahalanobis distance have been used to achieve the best results. A detailed description of metrics is provided in [41].

4.2. Design of experiment

We performed verification by comparing the test image with a set of corresponding images. The dataset has been divided into test and training subsets. The test subset contained one frontal image with a neutral facial expression taken from each person, while the training subset contained all the remaining images.

The training subset was required for computing a threshold for face verification and for learning classifiers for facial expressions. The test subset was used for validating the performance of the dataset and algorithms. Three types of experiments were performed to validate the dataset:

1. The experiment involving the entire dataset, between a frontal face image from the test subset and other images of the same as well as other subjects from the training subset;
2. The frontal face verification, where a frontal face image from the test subset was compared with frontal face images of the same as well as other subjects from the training subset;
3. The face recognition with various head positions, where a frontal face image from the test subset was compared with face images presenting the head in different positions of the same as well as other subjects from the training subset.

The quantitative assessment of the performance of the dataset and algorithms is based on known performance metrics including equal error rate, false match rate [47] and false non-match rate [48]. The equal error rate represents the value of algorithm threshold for which the proportion

of false matches is the same as false non-matches ($FNMR = FMR$). The *false match rate* (FMR) is a rate at which a biometric process mismatches biometric signals from two distinct individuals as coming from the same individual. The *false non-match rate* (FNMR) is a rate at which a biometric matcher mistakenly categorizes two signals from the same individual as being from different individuals. In this study, we have used FMR1000 which refers to the lowest FNMR for $FMR \leq 0.1\%$ and ZeroFMR, as a reference to the lowest FNMR for $FMR = 0\%$. *Receiver operating characteristics* (ROC) [49] graphs are also provided.

5. Baseline results and discussion

In this section, we present the results of the experiments using the presented database. Two main experiments were performed to show general usability of the dataset as well as to show a change of results after a year. The results are arranged in two main groups. The first part presents the results of experiments performed on the initial database while the second part consists of the results of experiments performed on the initial database together with the results collected after a year. Both parts include three evaluation tests performed according to the scenarios described in Subsection 4.2.

The results are summarized in tables and graphs. The values of recognition rates have been calculated accordingly.

Face descriptors have been calculated for different values of parameters. The HOG operator enables to set four main parameters – block size, cell size, the number of orientation histogram bins and the number of overlapping cells between adjacent blocks with initial values of 2×2 pixels, 8×8 pixels and 9, respectively. LBP can be fine-tuned with three main parameters, namely the number of neighbours, radius and cell size, with initial values of 8 pixels, 1 pixel and a size of an image, respectively. The third descriptor, LDP, is well adjusted to encode directive pattern features from local derivative variation. To optimize the facial descriptor, three parameters – derivative order, direction and patch size – with initial values of 2nd order, 4 directions and 16 pixels, are used. All the results presented in this paper have achieved the maximum for optimal values of parameters.

5.1. Initial dataset experiment

The initial dataset including thermal face images of 30 subjects has been evaluated in three experiments. The numerical results of experiments are presented in Tables 2–4 and their visual presentation is shown in Fig. 3. The results of experiments based on the entire initial database,

Table 2. Values of EER, FMR1000 and ZeroFMR for the recognition experiment based on the initial database.

Performance measure	Descriptor		
	HOG	LBP	LDP
EER [%]	8.68	4.54	5.41
FMR1000 [%]	76.45	87.19	87.6
ZeroFMR [%]	75.62	86.36	85.54
Metric	Spear.	City	Spear.

the frontal images as well as the face images representing different head positions are presented in Table 2, Table 3 and Table 4, respectively.

The outcome of the first experiment involving all facial images from the dataset is presented in Table 2. The biggest values of ZeroFMR are achieved using LBP as the feature descriptor and City distance as the matching method. Both LDB and LBP have achieved over 85% of accuracy.

The results of the second experiment involving frontal-face images only are presented in Table 3. The biggest values of ZeroFMR are achieved using LBP as the feature descriptor and Spearman distance as the matching method. The highest recognition rate is over 97%, however it should be noticed, that all the images considered during this experiment showed the subjects looking directly at the camera with neutral face expressions.

Table 3. Values of EER, FMR1000 and ZeroFMR for the recognition experiment based on the frontal images.

Performance measure	Descriptor		
	HOG	LBP	LDP
EER [%]	3.06	0.72	3.04
FMR1000 [%]	90.82	98.47	91.33
ZeroFMR [%]	88.27	97.45	90.82
Metric	City	Spear.	Spear.

The results of experiments on face images representing different head positions are presented in Table 4. The maximum value of ZeroFMR achieved during this experiment is significantly lower than that achieved during the previous two, up to 70%. Various head positions cause difficulties for feature-based descriptors when compared with frontal-face images, mainly due to a smaller number of corresponding features between the test and training samples.

Table 4. Values of EER, FMR1000 and ZeroFMR for the recognition experiment based on the face images representing different head positions.

Performance measure	Descriptor		
	HOG	LBP	LDP
EER [%]	29.46	32.31	29.96
FMR1000 [%]	14.29	27.68	19.64
ZeroFMR [%]	12.5	24.11	15.18
Metric	Cos	Spear.	Cos

ROC curves and graphs of equal error rates are shown in Fig. 3. EER lines are marked in violet and indicate the balance point between true positive and false positive rates.

The presented results of the three types of experiments indicate that the performance of facial recognition algorithms varies according to the types of experiments performed and the applied descriptor and metrics. The biggest values of recognition rates were obtained for the frontal face experiment. The performance assessed with the entire dataset achieved 86.36% (ZeroFMR), which gives more than a 10% decrease comparing with the frontal face experiment. According to the values of ZeroFMR and FMR1000, the highest and the lowest recognition rates were achieved by LBP and HOG, respectively.

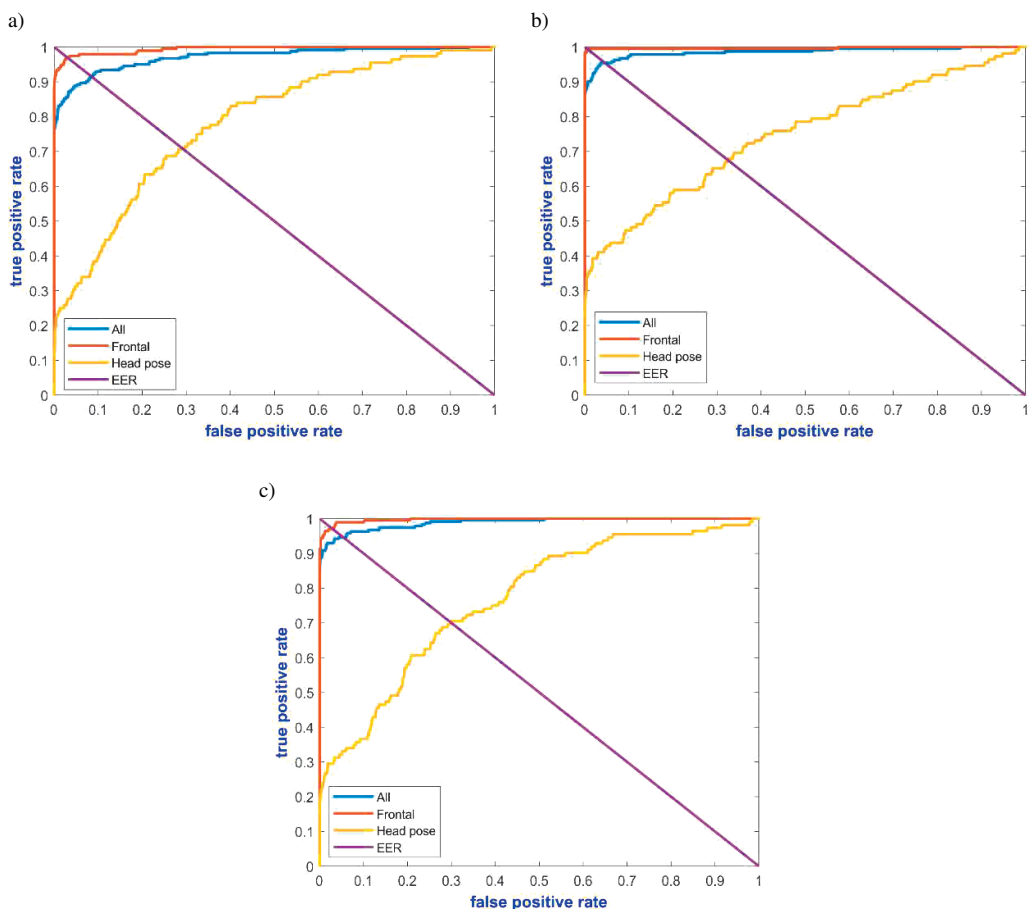


Fig. 3. ROC curves and EER lines of (a) HOG, (b) LBP and (c) LDP for the frontal-face re-identification experiment.

5.2. Repeated dataset experiment

Since aging influences the visible face recognition task, it is justified to investigate the impact of aging on the thermal face recognition. Both human face appearance and its physical properties change during the lifetime. The changes include thickness of skin, emissivity and temperature distribution. All those factors may affect the face recognition performance.

The database provides two corresponding sets of images acquired with a year interval. This data can facilitate the investigations of the aging impact on the thermal face recognition system.

The results of re-identification experiment using two sets of biometric samples collected with an interval of a year are shown in Fig. 4, with their values presented in Table 5. The best value of ZeroFMR calculated based on samples collected after a year are achieved for LDP and the correlation distance. However, the absolute value achieved is 41.23%, which is more than a 60% decrease, comparing with the results obtained based on the initial database. A noticeable decrease of performance shows that the heat emission changed due to various factors.

The results of repeated dataset experiment showed that the face representation in the long-wavelength infrared spectrum changes during time significantly. It requires further investigations

Table 5. Values of EER, FMR1000 and ZeroFMR for the recognition experiment for the frontal images (after a year).

Performance measure	Descriptor		
	HOG	LBP	LDP
EER [%]	27.61	27.8	24.95
FMR1000 [%]	26.32	40.26	50.65
ZeroFMR [%]	10.71	25.97	41.23
Metric	Spear.	Spear.	Corr.

to provide a detailed overview of all the aspects connected with this change. The recognition rates calculated during the experiment on the basis of images collected after a year are significantly lower than the respective initial results. Moreover, over 60% decrease of the recognition rate value creates a challenge for datasets and algorithms. Analyses of ZeroFMR and FMR1000 values indicate that the highest and the lowest recognition rates were achieved by LDP with the correlation distance and HOG with the Spearman metric, respectively.

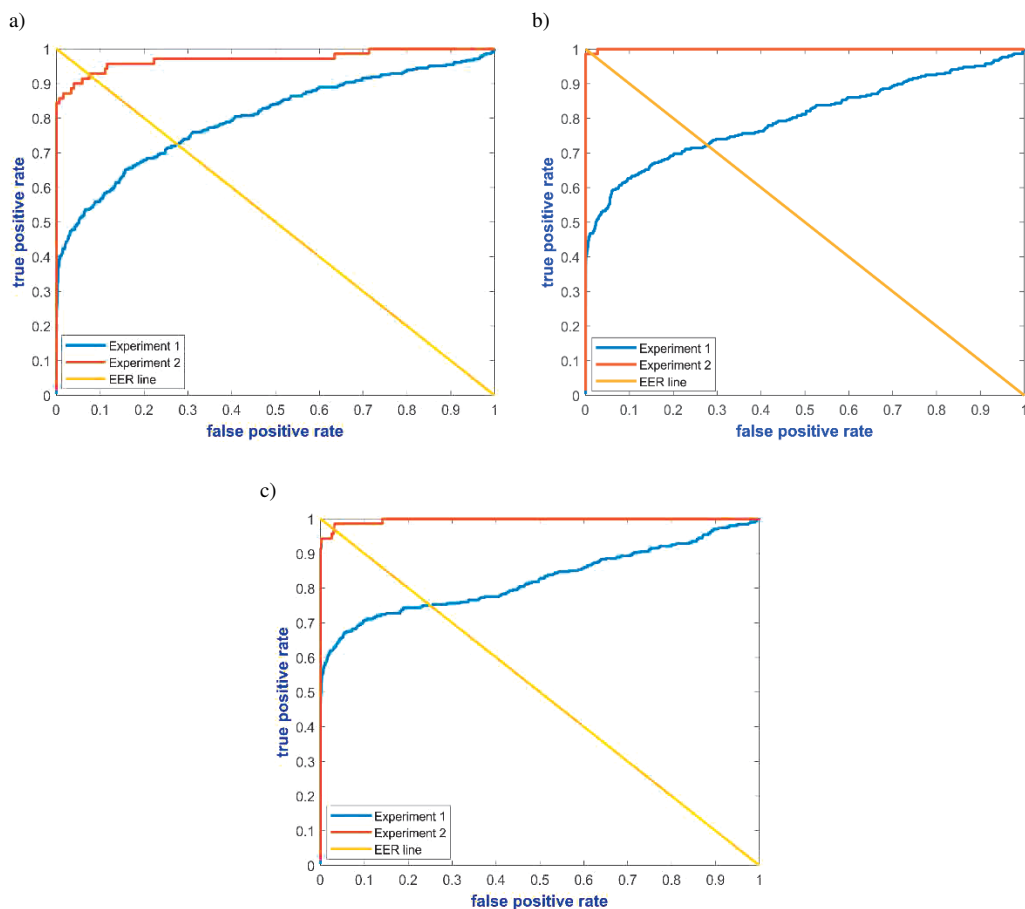


Fig. 4. ROC curves and EER lines of (a) HOG, (b) LBP and (c) LDP for the frontal-face re-identification experiment.

6. Conclusions

We have proposed a dataset of thermal facial images aimed at facilitating development and validation of an algorithm for thermal face recognition and thermal expression recognition. The dataset consists of a variety of neutral thermal images in various poses as well as a set of facial images with different expressions. Collection of the dataset was repeated after a year from the initial acquisition in order to provide information for investigations of the impact of aging. This dataset can be used for various purposes ranging from thermal face recognition to thermal expression recognition.

To evaluate applicability of the database, various scenarios of face re-identification experiments were performed. We present the baseline results of processing using state-of-the-art facial descriptors combined with a set of different distance metrics. Three selected local descriptors: a histogram of oriented gradients, local binary patterns and local derivative patterns have been used to validate the database in three types of experiments showing its performance for various tasks. The frontal face verification task was performed twice to show the impact of aging. The cross-check experiment involving data acquired twice: initially and after a year, showed a significant decrease of recognition rate.

Acknowledgements

This project has been funded by the European Union's Horizon 2020 research and innovation programme under the grant agreement No 700259.

The anonymized WAT thermal face dataset is available online on request [50]. The authors would like to thank all the subjects who participated in the experiments.

References

- [1] Kong, S., Heo, J., Abidi B., Paik, J., Abidi M. (2005). Recent advances in visual and infrared face recognition – a review. *Pattern Recognition*, 47(9), 2807–2824.
- [2] Abate, A.F., Nappi, M., Riccio, D., Sabatino, G. (2007). 2D and 3D face recognition: A survey. *Pattern Recogn. Lett.*, 28, 1885–1906.
- [3] Adini, Y., Moses, Y., Ullman, S. (1997). Face Recognition: The Problem of Compensating for Changes in Illumination Direction. *IEEE Trans. Pattern Anal. Mach. Intell.*, 19, 721–732.
- [4] Zhang, X., Gao, Y. (2009). Face recognition across pose: A review. *Pattern Recogn.*, 42, 2876–2896.
- [5] Bowyer, K.W., Kyong, C., Flynn, P. (2006). A survey of approaches and challenges in 3D and multi-modal 3D+2D face recognition. *Comput. Vis. Image Und.*, 101, 1–15.
- [6] Ghiass, R.Z., Arandjelović, O., Bendada, A., Maldague, X. (2014). Infrared face recognition: A comprehensive review of methodologies and databases. *Pattern Recogn.*, 47, 2807–2824.
- [7] Lettington, A.H., Hong, Q.H. (1993). An objective MRTD for discrete infrared imaging systems. *Meas. Sci. Technol.*, 4, 1106–1110.
- [8] Lahiri, B.B., Bagavathiappan, S., Jayakumar, T., Philip, J. (2012). Medical applications of infrared thermography: A review. *Infrared Physics & Technology*, 55, 221–235.
- [9] Hackforth, H.L. (1963). *Infrared Radiation*. WNT, Warsaw.
- [10] Vollmer, M., Mollmann, K.P. (2010). *Infrared thermal imaging: Fundamentals, Research and Applications*. Wiley-VCH.

- [11] Costello, J.T., McInerney, C.D., Bleakley, C.M., Selfe, J., Donnelly, A.E. (2012). The use of thermal imaging in assessing skin temperature following cryotherapy: a review. *Journal of Thermal Biology*, 37, 103–110.
- [12] Equinox Corp. Equinox Human Identification at a Distance Database. <http://www.equinoxsensors.com/products/HID.html>. (Accessed Mar. 31, 2017).
- [13] Grgic, M., Delac, K., Grgic, S. (2011). SCface – surveillance cameras face database. *Multimed. Tools Appl.*, 51, 863–879.
- [14] Espinosa-Duró, V., Faundez-Zanuy, M., Mekyska, J., Carl Database. Signal Processing Laboratory. <http://splab.cz/en/download/databaze/carl-database> (2017). (Mar. 31, 2017).
- [15] Espinosa-Duró, V., Faundez-Zanuy, M., Mekyska, J. (2013). A New Face Database Simultaneously Acquired in Visible, Near-Infrared and Thermal Spectrums. *Cognitive Computation*, 5, 119–135.
- [16] Hammoud, R.I. OTCBVS Benchmark Dataset Collection. <http://vcipl-okstate.org/pbvs/bench/>. (2017). (Accessed Apr. 10, 2017).
- [17] Wright, D.. Data Sets. Computer Vision Research Laboratory, Department of Computer Science and Engineering, University of Notre Dame. <https://sites.google.com/a/nd.edu/public-cvrl/data-sets>. (2017) (Accessed Apr. 19, 2017)
- [18] Ghiass, R.S., Arandjelović, O., Bendada, A., Maldague, X. (2013). Illumination-invariant face recognition from a single image across extreme pose using a dual dimension AAM ensemble in the thermal infrared spectrum. *The 2013 International Joint Conference on Neural Networks (IJCNN)*.
- [19] Wang S., et. al. (2010). A Natural Visible and Infrared Facial Expression Database for Expression Recognition and Emotion Inference. *IEEE Transactions on Multimedia*, 12(7).
- [20] Jackson, J.E. (1991). *A User's Guide to Principal Components*. Wiley, New York.
- [21] Yu, H., Yang, J. (2001). A direct LDA algorithm for high-dimensional data – with application to face recognition. *Pattern Recogn.*, 34, 2067–2070.
- [22] Comon, P. (1994). Independent component analysis, A new concept? *Signal Process.*, 36, 287–314.
- [23] Ojala, T., Pietikäinen, M., Harwood, D. (1994). Performance evaluation of texture measures with classification based on Kullback discrimination of distributions. *IEEE*.
- [24] Ojala, T., Pietikäinen, M., Harwood, D. (1996). A comparative study of texture measures with classification based on feature distributions. *Pattern Recogn.*, 29, 51–59.
- [25] Zou, J., Ji, Q., Nagy, G. (2007). A Comparative Study of Local Matching Approach for Face Recognition. *IEEE T. Image Process.*, 16, 2617–2628.
- [26] Hermosilla, G., Ruiz-del-Solar, J., Verschae, R., Correa, M. (2009). Face Recognition using Thermal Infrared Images for Human-Robot Interaction Applications: A Comparative Study. *Robotics Symposium (LARS), 2009 6th Latin American*.
- [27] Chen, J., Shan, S., He, C., Zhao, G., Pietikainen, M., Chen, X., Gao, W. (2010). WLD: A Robust Local Image Descriptor. *IEEE T. Pattern Anal.*, 32, 1705–1720.
- [28] Bay, H., Ess, A., Tuytelaars, T., Van Gool, L. (2008). *SURF: Speeded up Robust Features*. Springer, Berlin, Heidelberg.
- [29] Lowe, D.G. (2004). Distinctive Image Features from Scale-Invariant Keypoints. *Int. J. Comput. Vision*, 60, 91–110.
- [30] McConnell, R.K. (1986). Method of and apparatus for pattern recognition. *US Patent US4567610 A*.
- [31] Dalal, N., Triggs, B. (2005). Histograms of oriented gradients for human detection. *IEEE Computer Vision and Pattern Recognition*.
- [32] Déniz, O., Bueno, G., Salido, J., De la Torre, F. (2011). Face recognition using Histograms of Oriented Gradients. *Pattern Recogn. Lett.*, 32, 1598–1603.

- [33] Calvillo, A.D., Vazquez, R.A., Ambrosio, J., Waltier, A. (2016). *Face Recognition Using Histogram Oriented Gradients*. Springer.
- [34] Song, F., Tan, X., Liu, X., Chen, S. (2014). Eyes closeness detection from still images with multi-scale histograms of principal oriented gradients. *Pattern Recogn.*, 47, 2825–2838.
- [35] Tan, X., Triggs, B. (2010). Enhanced local texture feature sets for face recognition under difficult lighting conditions. *IEEE T. Image Process.*, 19, 1635–1650.
- [36] Ahonen, T., Pietikainen, M. (2007). Soft histograms for local binary patterns. *Finnish Signal Processing Symposium*, 1–4.
- [37] Heikkila, M., Pietikainen, M., Schmid, C. (2009). Description of interest regions with local binary patterns. *Pattern Recogn.*, 42, 425–436.
- [38] Zhang, W., Shan, S., Zhang, H., Gao, W., Chen, X. (2005). *Multi-resolution histograms of local variation patterns (MHLVP) for robust face recognition*. Springer.
- [39] Zhang, W., Shan, S., Zhang, H., Gao, W., Chen, X. (2005). Local gabor binary pattern histogram sequence (LGBPHS): A novel non-statistical model for face representation and recognition. *ICCV Tenth IEEE International Conference on Computer Vision*.
- [40] Zhang, B., Gao, Y., Zhao, S. (2010). Local Derivative Pattern Versus Local Binary Pattern: Face Recognition With High-Order Local Pattern Descriptor. *IEEE T. Image Process.*, 19, 533–544.
- [41] Deza, E., Deza, M.M. (2006). *Dictionary of Distances*. Elsevier.
- [42] Yin, S., Dai, X., Ouyang, P., Liu, L., Wei, S. (2014). A Multi-Modal Face Recognition Method Using Complete Local Derivative Patterns and Depth Maps. *Sensors*, 14, 19561–19581.
- [43] Ren, H., Sun, J., Hao, Y., Yan, X., Liu, X. (2014). Uniform Local Derivative Patterns and Their Application in Face Recognition. *Journal of Signal Processing Systems*, 74, 405–416.
- [44] Zhou, H.X., Lai, R., Liu, S.Q., Jiang, G. (2005). New improved nonuniformity correction for infrared focal plane arrays. *Optics Communications*, 245, 49–53.
- [45] Lim, J.S., (1990). *Two-Dimensional Signal and Image Processing*. Englewood Cliffs, NJ, Prentice Hall.
- [46] Jones, P.V.J. (2004). Robust Real-Time Face Detection. *International Journal of Computer Vision*.
- [47] False Match Rate. *Computational Methods in Biometric Authentication. Information Science and Statistics*. Springer, London.
- [48] Schuckers, M.E. (2010). False Non-Match Rate. *Computational Methods in Biometric Authentication. Information Science and Statistics*. Springer, London.
- [49] Tan, P.N. (2009). Receiver Operating Characteristic. *Encyclopedia of Database Systems*. Springer, Boston, MA.
- [50] WAT thermal face database. http://safe.wat.edu.pl/?page_id=17. (Accessed Feb. 13, 2018).